Revision of 12 Feb. 1998

Measurement of a small atmospheric ν_μ/ν_e ratio

The Super-Kamiokande Collaboration

Y.Fukuda[a], T. Hayakawa[a], E. Ichihara[a], K. Inoue[a], K. Ishihara[a], H. Ishino[a], Y. Itow[a], T. Kajita[a], J. Kameda[a], S. Kasuga[a], K. Kobayashi[a], Y. Kobayashi[a], Y. Koshio[a], K. Martens[a], M. Miura[a], M. Nakahata[a], S. Nakayama[a], A. Okada[a], M. Oketa[a], K. Okumura[a], M. Ota[a], N. Sakurai[a], M. Shiozawa[a], Y. Suzuki[a], Y. Takeuchi[a], Y. Totsuka[a], S. Yamada[a], M. Earl[b], A. Habig[b], J. T. Hong[b], E. Kearns[b], S. B. Kim[b,1], M. Masuzawa[b,2], M. D. Messier[b], K. Scholberg[b], J. L. Stone[b], L. R. Sulak[b], C. W. Walter[b], M. Goldhaber[c], T. Barszczak[d], W. Gajewski[d], P. G. Halverson[d,3], J. Hsu[d], W. R. Kropp[d], L. R. Price[d], F. Reines[d], H. W. Sobel[d], M. R. Vagins[d], K. S. Ganezer[e], W. E. Keig[e], E. W. Ellsworth[f], S. Tasaka[g], J. W. Flanagan[h,2], A. Kibayashi[h], J. G. Learned[h], S. Matsuno[h], V. Stenger[h], D. Takemori[h], T. Ishii[i], J. Kanzaki[i], T. Kobayashi[i], K. Nakamura[i], K. Nishikawa[i], Y. Oyama[i], A. Sakai[i], M. Sakuda[i], O. Sasaki[i], S. Echigo[j], M. Kohama[j], A. T. Suzuki[j], T. J. Haines[k,d], E. Blaufuss[l], R. Sanford[l], R. Svoboda[l], M. L. Chen[m], Z. Conner[m,4], J. A. Goodman[m], G. W. Sullivan[m], M. Mori[n,5], F. Goebel[o,6], J. Hill[o], C. K. Jung[o], C. Mauger[o], C. McGrew[o], E. Sharkey[o], B. Viren[o], C. Yanagisawa[o], W. Doki[p], T. Ishizuka[p,7], Y. Kitaguchi[p], H. Koga[p], K. Miyano[p], H. Okazawa[p], C. Saji[p], M. Takahata[p], A. Kusano[q], Y. Nagashima[q], M. Takita[q], T. Yamaguchi[q], M. Yoshida[q], M. Etoh[r], K. Fujita[r], A. Hasegawa[r], T. Hasegawa[r], S. Hatakeyama[r], T. Iwamoto[r], T. Kinebuchi[r], M. Koga[r], T. Maruyama[r], H. Ogawa[r], M. Saitoh[r], A. Suzuki[r], F. Tsushima[r], M. Koshiba[s], M. Nemoto[t], K. Nishijima[t], T. Futagami[u], Y. Hayato[u], Y. Kanaya[u], K. Kaneyuki[u], Y. Watanabe[u], D. Kielczewska[v,d,8], R. Doyle[w], J. George[w], A. Stachyra[w], L. Wai[w], J. Wilkes[w], K. Young[w]

[a] *Institute for Cosmic Ray Research, University of Tokyo, Tanashi, Tokyo 188-8502, Japan*
[b] *Department of Physics, Boston University, Boston, MA 02215, USA*
[c] *Physics Department, Brookhaven National Laboratory, Upton, NY 11973, USA*
[d] *Department of Physics and Astronomy, University of California, Irvine Irvine, CA 92697-4575, USA*
[e] *Department of Physics, California State University, Dominguez Hills, Carson, CA 90747, USA*
[f] *Department of Physics, George Mason University, Fairfax, VA 22030, USA*
[g] *Department of Physics, Gifu University, Gifu, Gifu 501-1193, Japan*
[h] *Department of Physics and Astronomy, University of Hawaii, Honolulu, HI 96822, USA*
[i] *Institute of Particle and Nuclear Studies, High Energy Accelerator Research Organization (KEK), Tsukuba, Ibaraki 305-0801, Japan*
[j] *Department of Physics, Kobe University, Kobe, Hyogo 657-8501, Japan*
[k] *Physics Division, P-23, Los Alamos National Laboratory, Los Alamos, NM 87544, USA*
[l] *Physics Department, Louisiana State University, Baton Rouge, LA 70803, USA*
[m] *Department of Physics, University of Maryland, College Park, MD 20742, USA*
[n] *Department of Physics, Miyagi University of Education, Sendai, Miyagi 980-0845, Japan*
[o] *Physics Department, State University of New York, Stony Brook, NY 11794-3800, USA*

[1] Present address: Department of Physics, Seoul National University, Seoul 151-742, Korea
[2] Present address: Accelerator Laboratory, High Energy Accelerator Research Organization (KEK)
[3] Present address: NASA, JPL, Pasadena, CA 91109, USA
[4] Present address: Enrico Fermi Institute, University of Chicago, Chicago, IL 60637 USA
[5] Present address: Institute for Cosmic Ray Research, University of Tokyo
[6] Present address: Deutsches Elektronen-Synchrotron DESY, Hamburg, Germany
[7] Present address: Dept. of System Engineering, Shizuoka University Hamakita, Shizuoka 432-8561, Japan

[8] Supported by the Polish Committee for Scientific Research.

[p] Department of Physics, Niigata University, Niigata, Niigata 950-2181, Japan
[q] Department of Physics, Osaka University, Toyonaka, Osaka 560-0043, Japan
[r] Department of Physics, Tohoku University, Sendai, Miyagi 980-8578, Japan
[s] The University of Tokyo, Tokyo 113-0033, Japan
[t] Department of Physics, Tokai University, Hiratsuka, Kanagawa 259-1292, Japan
[u] Department of Physics, Tokyo Institute for Technology, Meguro, Tokyo 152-8551, Japan
[v] Institute of Experimental Physics, Warsaw University, 00-681 Warsaw, Poland
[w] Department of Physics, University of Washington, Seattle, WA 98195-1560, USA

Abstract

From an exposure of 25.5 kiloton-years of the Super-Kamiokande detector, 900 muon-like and 983 electron-like single-ring atmospheric neutrino interactions were detected with momentum $p_e > 100$ MeV/c, $p_\mu > 200$ MeV/c, and with visible energy less than 1.33 GeV. Using a detailed Monte Carlo simulation, the ratio $(\mu/e)_{DATA}/(\mu/e)_{MC}$ was measured to be $0.61 \pm 0.03(stat.) \pm 0.05(sys.)$, consistent with previous results from the Kamiokande, IMB and Soudan-2 experiments, and smaller than expected from theoretical models of atmospheric neutrino production.

Introduction

Atmospheric neutrinos are the decay products of hadronic showers produced by cosmic ray interactions in the atmosphere. In recent years, the ratio $R \equiv (\mu/e)_{DATA}/(\mu/e)_{MC}$ has been measured to study the atmospheric neutrino flavor ratio $(\nu_\mu + \overline{\nu}_\mu)/(\nu_e + \overline{\nu}_e)$; the ratio of data to Monte Carlo is taken to cancel uncertainties in the neutrino flux and cross sections. Here, (μ/e) denotes the ratio of the numbers of μ-like to e-like neutrino interactions observed in the data or predicted by the Monte Carlo (MC). The expected value for R is unity if there is agreement between the experiment and the theoretical prediction. The water Cherenkov detectors Kamiokande [1] and IMB [2] have observed a statistically significant low value of R for "sub-GeV" events with lepton energies of about 1 GeV or less. The NUSEX [3] and Fréjus [4] experiments have reported no deviation from unity, but with smaller data samples. Recently the Soudan-2 experiment [7] has also observed an R value smaller than unity. Kamiokande [5] also observed a smaller μ/e ratio in the "multi-GeV" energy range, as well as a dependence of this ratio on the zenith angle, and hence the neutrino travel distance. The small value of the ratio and the zenith angle dependence suggest that neutrino oscillations may be responsible for these results.

This letter presents the first measurement of the μ/e ratio using the Super-Kamiokande detector. The data were restricted to the sub-GeV range, which comprises contained events with visible energy less than 1.33 GeV and electron (muon) momentum greater than 100 MeV/c (200 MeV/c); these criteria match the definition used by Kamiokande.[9] We carried out two independent analyses (A and B) whose results were consistent with each other, confirming the validity of the methods used.

[9] This analysis has also been performed with a minimum p_μ of 300 MeV/c and $p < 1.5$ GeV, corresponding to the kinematic cuts used in prior analyses by the IMB experiment [2]; results were very similar.

Super-Kamiokande detector

Super-Kamiokande is a 50-kiloton water Cherenkov detector located near the Kamioka ande detector, in the Mozumi mine of the Kamioka Mining Company in Gifu prefecture, Japan. It lies at a mean overburden of 2,700 meters-water-equivalent below the peak of Mt. Ikenoyama. The inner detector comprises 11,146 Hamamatsu R3600 50-cm diameter photomultiplier tubes (PMT), viewing a cylindrical volume of pure water 16.9 m in radius and 36.2 m high. The 50-cm PMTs were specially designed[6] to have good single photoelectron (p.e.) response, with timing resolution 2.5 ns RMS. An outer layer of water 2.6 to 2.75 m thick completely surrounds the inner detector to passively shield against radioactivity from the surrounding rock. The two detector regions are optically separated by a pair of opaque sheets which enclose a dead region 55 cm in thickness. The outer detector is instrumented with 1,885 outward-facing Hamamatsu R1408 20-cm PMTs. In order to increase light collection, 60 cm × 60 cm wavelength shifters[8] were attached to the outer PMTs, and all surfaces of the outer detector were covered with reflective white DuPont Tyvek material. The outer detector data were used to identify incoming cosmic rays and exiting muons from neutrino interactions.

Both inner and outer PMT signals were processed by asynchronous, self-triggering circuits that record the time and charge of each PMT hit over a threshold. The inner PMT signals were digitized with custom Analog Timing Modules (ATMs)[9] which provide 1.2 μs range at 0.3 ns resolution in time and 550 pC range at 0.2 pC resolution (1/10 p.e.) in charge for each PMT. The ATM has automatically switched dual channels to provide deadtime-free data acquisition. The outer PMT signals were processed with custom charge-to-time conversion modules, which output timing pulses of width linearly proportional to the integrated charge of the PMT pulse. These signals were digitized with LeCroy 1877 multi-hit TDCs using 16 μs full range.

A trigger was formed by the coincidence of at least 30 PMT hits in a 200 ns window, over a threshold of about 1/4 p.e. per PMT. This trigger condition corresponds to the mean number of hit PMTs for a 5.7 MeV electron. The trigger rate was 10-12 Hz. The trigger rate due to cosmic ray muons was 2.2 Hz. Digitized data were saved at a total rate of 12 GB per day.

Water transparency was measured using a dye laser and CCD camera, and found to be about 100 m at wavelength 420 nm. During the time period described here (approximately 17 months of detector operation), water transparency was monitored continuously by cosmic-ray muons; the average effective attenuation length for Cherenkov light increased by 25%, due to improvement in water clarity resulting from operation of the water purification system.

The calibration of digitized PMT data to number of p.e.s and arrival time was performed by offline processes directly linked to the detector data stream via local network. Both of the independent analyses began with the same calibrated data. Each analysis independently estimated the conversion from p.e. to visible energy (E_{vis}), which is defined as the energy of an electromagnetic shower which produces an equivalent amount of Cherenkov light. Approximately 9 p.e.s were measured for one MeV of visible energy. The accuracy of the absolute energy scale was estimated to be $\pm 2.4\%$ based on several calibration sources: cosmic ray through-going muons, stopping muons, muon-decay electrons, the invariant mass of π^0s produced by neutrino interactions, radioactive source calibration, and a 5-16 MeV electron LINAC. The estimated momentum resolution for electrons and muons is $2.5\%/\sqrt{E(GeV)} + 0.5\%$ and 3%, respectively.

Both analyses required the vertex of the neutrino interactions to be reconstructed inside a fiducial volume 2 m from the light barrier just outside the inner PMT plane. This comprised a concentric cylindrical volume 32.2 m high and 14.9 m in radius with a mass of 22.5 kilotons.

	Data	Monte Carlo			
		total	ν_e CC(q.e.)	ν_μ CC(q.e.)	NC
single-ring	1883	2030.5	720.1(562.4)	1185.0(921.4)	125.3
e-like	983	812.2	714.3(558.4)	18.6(4.5)	79.3
μ-like	900	1218.3	5.8(4.0)	1166.5(916.9)	46.0
multi-ring	784	759.2	182.1(46.6)	325.5(47.3)	251.6
total	2667	2789.7	902.2(609.0)	1510.5(968.7)	376.9

Table 1: Summary of the sub-GeV experimental data compared with the Monte Carlo estimation. Monte Carlo statistics have been normalized to the live time of the experimental data. "q.e." refers to quasi-elastic events.

	1 or more muon decays		2 or more muon decays	
	data	MC	data	MC
μ-like	$608/900 = 67.6 \pm 1.6\%$	$68.1 \pm 0.1 \pm 1.0\%$	$26/900 = 2.9 \pm 0.6\%$	$4.1 \pm 0.1 \pm 0.2\%$
e-like	$91/983 = 9.3 \pm 0.9\%$	$8.7 \pm 0.3 \pm 0.1\%$	$2/983 = 0.2 \pm 0.1\%$	$0.1 \pm 0.1 \pm 0.01\%$

Table 2: Percentages of events with muon decay in single-ring events. The first error value shown is statistical. For Monte Carlo, the second error value is from the estimated muon decay detection efficiency.

Analysis A

For analysis A, we used data from a 25.5 kiloton-years net exposure, collected during the period between May 1996 and October 1997. The main backgrounds for the observation of atmospheric neutrino events were cosmic ray muons and low-energy radioactivity in the detector. These two backgrounds were rejected by requiring no correlated hits in the outer detector and a minimum deposited energy of 30 MeV in the inner detector, respectively.

Starting from $\sim$ 400 million triggers, the data sample was reduced to about 12,000 events by applying the following requirements: (1) no significant outer detector activity (total number of hits less than 25, and no spatial cluster with more than 10 hits), (2) total charge collected in the inner detector $>$ 200 p.e.s, which corresponds to 22 MeV/ c for electrons and 190 MeV/ c for muons, (3) the ratio (maximum p.e. in any single PMT)/(total p.e.s) is less than 0.5, and (4) the time interval from the preceding event $>$ 100 μs, to reject electrons from stopping muon decays. Additional selection criteria were used to eliminate spurious events, such as those due to "flashing" PMTs that emit light from internal corona discharges. The selected events were hand-scanned by two independent scanners, to reject remaining background events. About

6,000 events were classified as fully-contained events, a large fraction of which were neutrino interactions with no charged particle exiting into the outer detector.

The vertex position of an event was determined using PMT hit times; the point which yielded the sharpest distribution of PMT times adjusted for the time of flight of Cherenkov light was defined as the vertex position. The vertex was reconstructed again after particle identification to correct for particle track length. The vertex resolution was estimated to be 30 cm for single-ring fully-contained events. The number of Cherenkov rings and their directions were determined automatically by a maximum-likelihood procedure. The efficiency for identifying quasi-elastic $\nu_e(\nu_\mu)$ events as single-ring was 93(95)%. The angular resolution for single-ring events was estimated to be 3 degrees. The momentum of a particle was determined from the total number of p.e.s within a 70° half-angle cone relative to the track direction, with corrections for light attenuation and PMT angular acceptance.

The particle identification of the final state lepton exploits systematic differences in the shape and the opening angle of Cherenkov rings produced by electrons and muons. Cherenkov rings from electromagnetic cascades exhibit more diffuse light distribution than those from muons. The opening angle of the Cherenkov cone, which depends on $\beta(\equiv v/c)$, was used to separate electrons and muons at low momenta. The validity of the method was confirmed by a beam test experiment at KEK[10]. Figure 1 shows distributions of the PID parameter (effectively a log-likelihood difference for the electron and muon hypotheses) for the data and for Monte Carlo single-ring events. If the PID parameter was positive (negative), the event was classified as e-like (μ-like). The misidentification probabilities for single-ring muons and electrons were estimated to be $0.5 \pm 0.1\%$ and $0.7 \pm 0.1\%$, using simulated charged-current (CC) quasi-elastic neutrino events. The identification efficiency was checked using cosmic-ray muons which stop in the detector and subsequently decay to electrons. The resulting misidentification probabilities for these muon and electron events were $0.4 \pm 0.1\%$ and $1.8 \pm 0.5\%$, respectively, in good agreement with the Monte Carlo estimates. This check was performed continuously during data-taking, and particle identification performance remained stable despite increasing water transparency.

There are several calculations of the expected atmospheric neutrino flux at the Super-Kamiokande site. The calculated flux of Ref. [11] was used for the Monte Carlo simulation of atmospheric neutrino interactions. The neutrino interaction model took into account quasi-elastic scattering [12], single-pion production [13], coherent pion production [14], and multi-pion production [15]. Propagation of produced leptons and hadrons was modeled using a GEANT [16]-based detector simulation, which included Cherenkov light production and propagation in water. Hadronic interactions were simulated by CALOR [17], except for pions with momentum less than 500 MeV/c, for which a special program [15] was developed, with cross-sections taken from the experimental results. For pions produced in ^{16}O nuclei, inelastic interactions, charge exchange, and absorption in the nuclei were also taken into account [15]. A sample equivalent to 10 years of detector operation was generated with the Monte Carlo simulator. This Monte Carlo sample was then passed through the same event filtering[10] and reconstruction as the experimental data.

From the initial 6,000 fully-contained events, 3,462 neutrino event candidates were reconstructed in the fiducial volume with $E_{vis} > 30$ MeV. We estimated that 83.0% of the total charged current interaction events in the fiducial volume were retained in the present sample. The sources of inefficiency were: non-fully-contained (9.3%), E_{vis} lower than 30 MeV (5.8%), reduction inefficiency (0.1%), and a small systematic bias toward fitting the vertex position outside

[10] The Monte Carlo was not hand scanned, except for selected samples for studies.

of the fiducial volume (2.1% and 1.5% for the e-like and μ-like events respectively).

To measure the μ/e ratio we required that there be only a single ring identified in the event. The sub-GeV kinematic requirements were: E_{vis} less than 1.33 GeV, and electron and muon momenta greater than 100 and 200 MeV/c, respectively. Table 1 summarizes the number of observed events and compares them with the Monte Carlo estimation. From these data, we obtained:

$$R \equiv (\mu/e)_{DATA}/(\mu/e)_{MC} = 0.61 \pm 0.03(stat.) \pm 0.05(sys.).$$

Sources of systematic uncertainty in R were estimated as follows: 5% from uncertainty in the predicted ν_μ/ν_e flux ratio, 3.5% from uncertainty in the CC neutrino interaction cross sections and nuclear effects in the H_2O target, 3% from the neutral current (NC) cross section, 0.5% from the uncertainty in pion propagation in water, 3% from single-ring event selection, 2% from particle identification, 1% from the absolute energy calibration, 0.6% from the vertex fit and fiducial volume cut, less than 0.5% from contamination by cosmic ray muons, flashing PMT events and neutron interactions in the detector, and 1.5% from statistical uncertainty in the Monte Carlo. Adding these errors in quadrature, the total systematic uncertainty is 8%.

The result using particle identification was checked with the rate of muon decays in the neutrino events. The detection efficiency for muon decay was estimated to be 80% for μ^+ and 63% for μ^- by a Monte Carlo study. These figures were confirmed with an accuracy of 1.5% using cosmic-ray stopping muons. The fraction of events with muon decays in the single-ring event sample is shown in Table 2, and is in good agreement with the Monte Carlo estimation, for both μ-like and e-like events. This supports the reliability of the particle identification and the Monte Carlo estimation of pion production.

Analysis B

An independent analysis of the Super-Kamiokande data was performed, to detect possible errors and provide a comparison of reduction and reconstruction techniques. The computer programs used were completely independent from Analysis A, as were the determinations of energy scale and systematic uncertainty. The common starting point for each analysis was the raw data with electronics calibration applied. The selection of the data sample was slightly different, and analysis B had an exposure of 25.8 kiloton-years.

In Analysis B, the initial set of events was obtained by applying the following requirements: (1) fewer than 10 PMT hits in the outer detector in a 200 ns window around the trigger time, (2) total charge collected in the inner detector > 100 p.e.s, within a 200 ns time window, (3) the ratio (maximum p.e.s in any single PMT) / (total p.e.s) was less than 0.4, (4) the time interval from the preceding event > 100 μs.

In the next stage of the analysis, a vertex point fit was done by χ^2 minimization of the difference between the PMT time and the time expected, based on light propagating from a vertex. The charge in a ± 20 ns window of residual time was required to be greater than 150 p.e.s. A second fit was applied for the hypothesis of a long cosmic ray muon; if the entry point had more than 2 outer detector tube hits within 20 m and ± 50 ns, the event was rejected.

Remaining flashing PMT events were removed by imposing requirements on the shape of the residual time distribution. In addition, a separate analysis was performed that rejected events with repetitive light patterns characteristic of specific flashing PMTs. In the final stage of the

reduction, a precise vertex and direction fit was applied. The vertex reconstruction had 40 cm resolution superimposed on an uncorrected shift of +43(-43) cm for electrons (muons).

These requirements resulted in 3,521 fully contained events within the fiducial volume. Among them, we visually identified 3 events caused by electronics noise, 1 flashing PMT event, and 1 event likely to be an entering cosmic ray muon; however, no events were removed based on scanning. This constituted a background of 0.2%, which was accounted for in the systematic uncertainty. Based on Monte Carlo studies we estimated that 85% of the total CC interaction events were retained in the sample: 80% from ν_μ and 95% from ν_e. There was a small systematic bias toward fitting the vertex position for electrons outside (2.7%) and muons inside (2.0%) of the fiducial volume.

Single-ring events were selected based on cuts using the azimuthal distribution of light which falls behind the Cherenkov cone of the track; events with azimuthal symmetry were considered single-ring, and those with asymmetry were considered multi-ring. Based on Monte Carlo studies, the percentage of quasi-elastic interactions in the sample selected by this algorithm was estimated to be 78% with a 93%(98%) efficiency for identifying quasi-elastic $\nu_e(\nu_\mu)$ events as single-ring.

Particle identification was performed using the vertex and direction from the final track fit and the distribution of PMT charge projected onto the track axis at the Cherenkov angle. The shape of this distribution was used to determine the particle type, primarily by measuring more projected charge behind the vertex for electromagnetic showers than for muons. The particle misidentification probabilities for quasi-elastic ν_μ and ν_e events were $1.4^{+1.6}_{-0.5}$% and $3.5^{+1.4}_{-1.5}$% respectively.

The momentum of the final state lepton was determined from the total number of p.e.s in a 20 ns window of residual time, taking into account the higher Cherenkov threshold for muons. The final data sample of single-ring events, within the same sub-GeV kinematic range defined in Analysis A, and with vertices in the fiducial volume, consisted of 1,041 μ-like events and 967 e-like events. The distributions of the particle identification parameter for data and Monte Carlo are shown in Figure 2.

A sample of Monte Carlo events was generated corresponding to 10.2 years of exposure, using the atmospheric ν_μ and ν_e flux predictions of Ref. [18] and the pion-production models of Rein and Seghal [13, 14] as adapted for use in the IMB experiment [19]. A second sample was generated using the same flux but following the pion-production model of Fogli and Nardulli [20, 21] as a check; essentially all results were found to agree with the first Monte Carlo sample within the estimates of systematic uncertainty. Both Monte Carlo samples used common code to track particles in water, generate Cherenkov light, and simulate the detector response. The Monte Carlo events were processed through the same analysis chain as the experimental data. The classification of data and Monte Carlo events is summarized in Table 3. Finally, we obtained $R = 0.65 \pm 0.03(stat.) \pm 0.05(sys.)$, in good agreement with analysis A.

Estimated contributions to the systematic uncertainty in R were as follows: 5% from the uncertainty in the predicted ν_μ/ν_e flux ratio, 3.5% from particle misidentification, 3.4% from the uncertainty in the CC neutrino cross section, 2.2% from the NC neutrino cross sections, 1.9% from single-ring selection, 1.8% from the energy calibration, 1.5% from fiducial volume determination, less than 0.5% from non-neutrino backgrounds contamination, and 1.5% from the statistical error in the Monte Carlo. These sum in quadrature to a total systematic uncertainty of 8.1%.

As in analysis A, the fraction of events with one or more muon decays was in good agreement

with Monte Carlo prediction. For e-like events, $8.4 \pm 0.9\%$ were found with one or more decay signals compared to the Monte Carlo prediction of $10.6 \pm 0.4(stat.) \pm 0.3(sys.)\%$. For μ-like events, $55.2 \pm 1.5\%$ were found with one or more decays and $2.3 \pm 0.5\%$ with two or more decays, compared with the Monte Carlo predictions of $55.7 \pm 0.5(stat.) \pm 1.7(sys.)\%$ and $3.3 \pm 0.2(stat.) \pm 0.1(sys.)\%$ respectively.

	Data	Monte Carlo			
		total	ν_e CC(q.e.)	ν_μ CC(q.e.)	NC
single-ring	2008	2185.9	724.1(610.7)	1306.6(1095.7)	155.2
e-like	967	821.1	696.0(587.7)	32.8(15.4)	92.4
μ-like	1041	1364.8	28.1(23.0)	1273.9(1080.3)	62.8
multi-ring	642	631.3	151.1(44.3)	246.2(25.2)	233.9
total	2650	2817.2	875.3(655.0)	1552.9(1120.9)	389.1

Table 3: Summary of sub-GeV events compared with Monte Carlo estimation, for 25.8 kiloton-years of Super-Kamiokande data processed by Analysis B.

Comparison of analyses

Livetime selection was slightly different for Analysis A and Analysis B; 95% of the livetime of each group was analyzed by the other. For runs analyzed by both groups, we found that 94% of the events in the final sample of Analysis A (both single and multi-ring) were also included in the final sample of Analysis B. Comparing the ring-counting algorithm of analysis A with the single-ring selection cuts of analysis B, we found that 90% of Analysis A events had the same classification in Analysis B. We compared reconstructed quantities for single-ring events commonly selected by both A and B. For these events the mean absolute difference in reconstructed vertex position was 84 cm parallel, and 18 cm perpendicular to the track direction. Reconstructed track directions agreed with a mean of angular difference of 2.5 degrees. The average difference in momentum ($\Delta P/P$) was 0.5%. Comparing particle identification, we found that 97% of Analysis A events agreed with the Analysis B classification as e-like or μ-like. These results are consistent with expectation based on the resolution and efficiencies of the software developed independently by the two analysis groups. Finally, we found that the systematic uncertainties estimated by each analysis were consistent with the differences in event reconstruction.

We note that μ/e ratios for data and Monte Carlo in Analysis A were smaller than those in Analysis B by 15% and 10%, respectively. The difference in the Monte Carlo ratios is primarily due to differences in the vertex fitting and single-ring selection. Using livetimes which did not completely overlap, Analysis A and B found R values which were different by 5.8%; however, if common runs were used the difference was 4.4%. This difference is consistent with the known differences in particle identification between the two analyses, the systematic error in R due to different analysis techniques only, and the Monte Carlo statistical error.

Results

Results from the two independent analyses agree well, not only in R but also in all other points of comparison. Thus, it would be difficult to explain the observed deviation of R from expectation in terms of unresolved mistakes in experimental data analysis. Since results from the two independent analyses are consistent, further discussion refers to results from analysis A.

In Figure 3, R is shown to have no strong dependence on D_{WALL}, the distance from the vertex to the nearest wall (even outside the fiducial volume at $D_{WALL} < 2$ m). There is no evidence for neutron or other background which could change $(\mu/e)_{DATA}$ near the edge of the fiducial volume. Based on the scanning of events near $D_{WALL} = 0$, we determined that the higher R value in the first bin was likely to be due to cosmic-ray muon background, but no significant muon background was observed for the other bins.

Figures 4(a) and (b) show the momentum distributions of the e-like and μ-like events, respectively. The systematic uncertainty in the absolute normalization of the Monte Carlo events is $\pm 25\%$: 20% from the uncertainty of the neutrino flux calculation and 15% from the neutrino interaction cross section. As a result, we cannot determine from these data alone whether the observed deviation of R from unity is due to an electron excess or a muon deficit. The shape of each distribution was consistent with Monte Carlo prediction; χ^2/d.o.f. was 2.9/12 for the e-like events and 12.2/12 for μ-like events. Figure 4(c) shows R as a function of momentum. It is consistent with a flat distribution within the statistical error.

For the sub-GeV single-ring sample, Monte Carlo studies showed the mean neutrino energy for CC interactions to be about 700 MeV for e-like events and 800 MeV for μ-like events; the mean angular correlation between the charged lepton and the neutrino was estimated to be 54° for muons and 62° for electrons. Figures 5(a) and (b) show the $\cos\Theta$ distributions for e-like and μ-like events, where Θ is the zenith angle of the particle direction. The $\pm 25\%$ error of normalization is also shown. The shape of the distribution was consistent with expectation for the e-like events (χ^2/d.o.f. = 6.5/4). However, it was worse (χ^2/d.o.f. = 18.6/4) for the the μ-like events. Figure 5(c) shows R binned by zenith angle. Using the two calculated fluxes[11, 18] and comparing the $(e\text{-like})_{MC}$, $(\mu\text{-like})_{MC}$, and $(\mu/e)_{MC}$ shapes for the five $\cos\Theta$ bins, we found that the two calculations had $\pm 2.2\%$ ($\pm 1.4\%$) difference for the e-like (μ-like) prediction. However, they had very similar $(\mu/e)_{MC}$ vs $\cos\Theta$ distributions. We conclude that any up-down systematic asymmetry in R from the uncertainty in the assumed flux model is less than $\pm 1\%$. We estimated that the measured energy was 3% higher for down-going compared to up-going particles by studying decay electrons from stopping cosmic ray muons. This gain asymmetry caused $\pm 0.1\%$ ($\pm 0.4\%$) up-down asymmetry in e-like (μ-like) events, implying an up-down asymmetry in R of $\pm 0.4\%$. The contamination of non-neutrino background, less than 0.5%, could have directional correlation and could cause a maximum of $\pm 1\%$ up-down systematic error. Adding these in quadrature, the systematic uncertainty in the up-down asymmetry in R is 1.5%. This systematic uncertainty is negligibly small compared with the statistical errors in Figure 5(c).

Conclusions

The first measurements of atmospheric neutrinos in the Super-Kamiokande experiment have confirmed the existence of a smaller atmospheric ν_μ/ν_e ratio than predicted. We obtained $R = 0.61 \pm 0.03(stat) \pm 0.05(sys)$ for events in the sub-GeV range. The Super-Kamiokande

detector has much greater fiducial mass and sensitivity than prior experiments. Given the relative certainty in this result, statistical fluctuations can no longer explain the deviation of R from unity.

We gratefully acknowledge the cooperation of the Kamioka Mining and Smelting Company. The Super-Kamiokande experiment was built and operated from funding by the Japanese Ministry of Education, Science, Sports and Culture, and the United States Department of Energy.

References

[1] K.S. Hirata *et al.*, Phys. Lett. **B205** (1988) 416;
K.S. Hirata *et al.*, Phys. Lett. **B280** (1992) 146.

[2] D. Casper *et al.*, Phys. Rev. Lett. **66** (1991) 2561;
R. Becker-Szendy *et al.*, Phys. Rev. **D46** (1992) 3720.

[3] M. Aglietta *et al.*, Europhys. Lett. **8** (1989) 611.

[4] K. Daum *et al.*, Z. Phys. **C66** (1995) 417.

[5] Y. Fukuda *et al.*, Phys. Lett. **B335** (1994) 237.

[6] A. Suzuki *et al.*, Nucl. Inst. and Meth. **A329** (1993) 299.

[7] W.W.M. Allison *et al.*, Phys. Lett. **B391** (1997) 491.

[8] R. Claus *et al.*, Nucl. Inst. and Meth. **A261** (1987) 540.

[9] T. Tanimori *et al.*, IEEE Trans. Nucl. Sci. **36** (1989) 497.

[10] S. Kasuga *et al.*, Phys. Lett. **B374** (1996) 238.

[11] M. Honda *et al.*, Phys. Rev. **D52** (1995) 4985;
M. Honda *et al.*, Phys. Lett. **B248** (1990) 193.

[12] C.H. Llewellyn Smith, Phys. Rep. **3** (1972) 261.

[13] D. Rein and L.M. Seghal, Ann. Phys. **133** (1981) 79.

[14] D. Rein and L.M. Seghal, Nucl. Phys. **B223** (1983) 29.

[15] M. Nakahata *et al.*, J. Phys. Soc. Jpn. **55** (1986) 3786.

[16] "GEANT Detector Description and Simulation Tool", CERN Program Library W5013 (1994).

[17] T.A. Gabriel *et al.*, IEEE Trans. Nucl. Sci 36, 1 (1989) 14.

[18] G. Barr *et al.*, Phys. Rev. **D39** (1989) 3532;
V. Agrawal *et al.*, Phys. Rev. **D53** (1996) 1314;
T.K. Gaisser and T. Stanev, Proc. 24th Int. Cosmic Ray Conf. (Rome) Vol. 1 (1995) 694.

[19] D. Casper, PhD. thesis, University of Michigan, 1990.

[20] G.L. Fogli and G. Nardulli, Nucl. Phys. **B160** (1979) 116.

[21] T. Haines, *et al.*, Phys. Rev. Lett. **57** (1986) 1986.

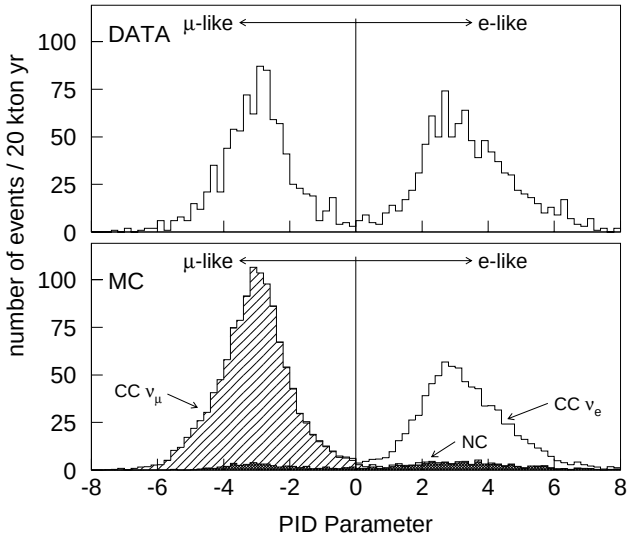

Figure 1: Distribution of the particle identification (PID) parameter for single-ring atmospheric neutrino events for both data and Monte Carlo samples in Analysis A. If the PID parameter of an event is positive (negative), the event is classified as e-like (μ-like). For the Monte Carlo, the contributions from charged current and the neutral current events are also shown.

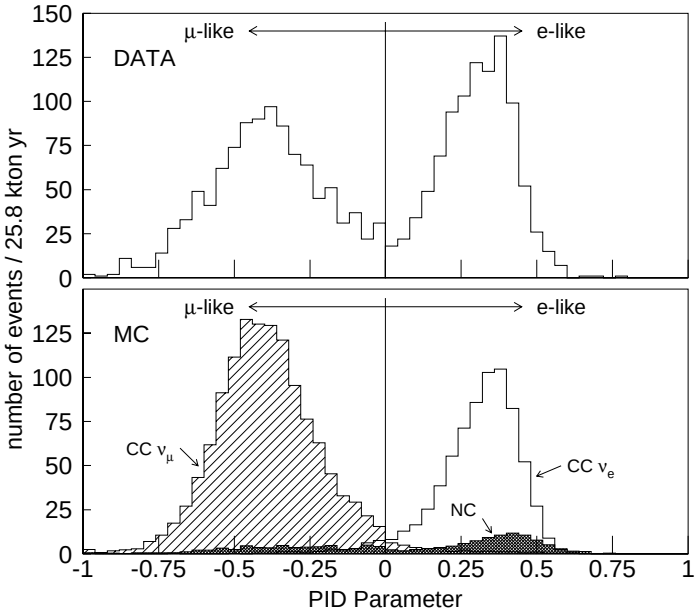

Figure 2: Distribution of the PID parameter used in Analysis B for μ-like events (PID < 0) and e-like events (PID > 0) in both data and Monte Carlo samples.

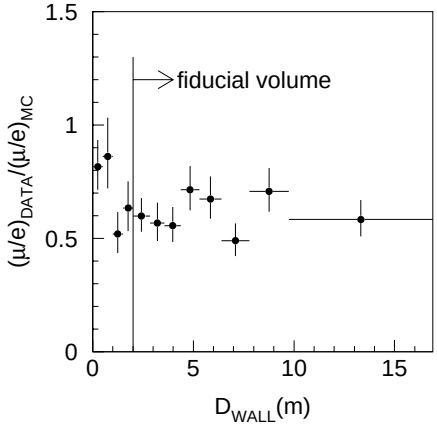

Figure 3: R as a function of D_{WALL}, the distance between the event vertex and inner detector wall. The region $D_{WALL} > 2$m is the fiducial volume.

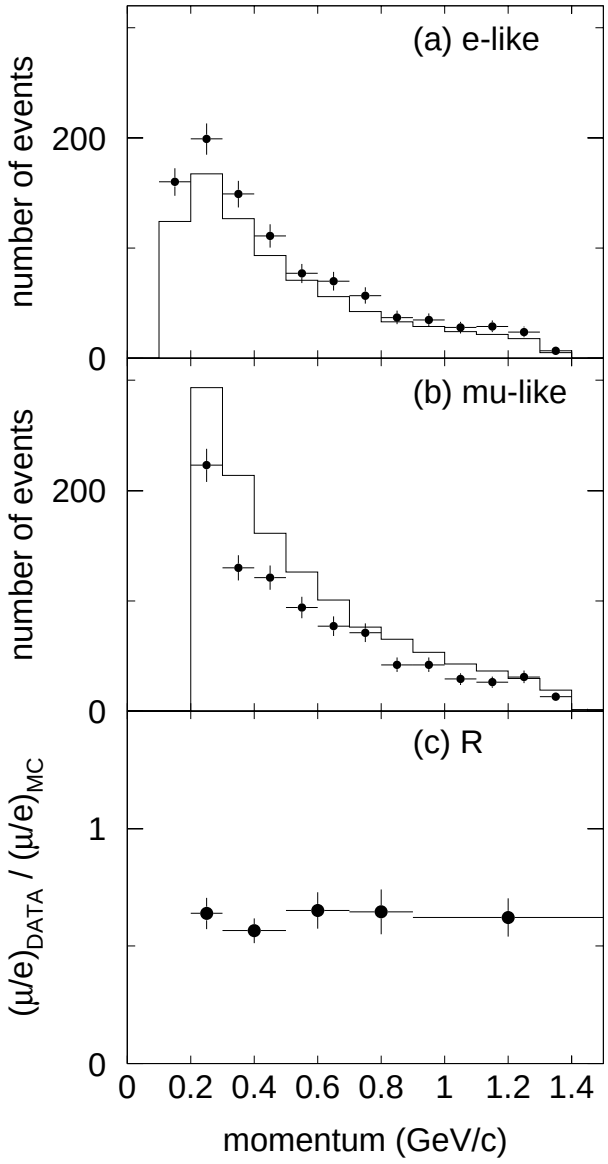

Figure 4: Momentum distributions for: (a) e-like events, (b) μ-like events, and (c) R. The histograms show the Monte Carlo prediction. Error bars represent statistical errors only.

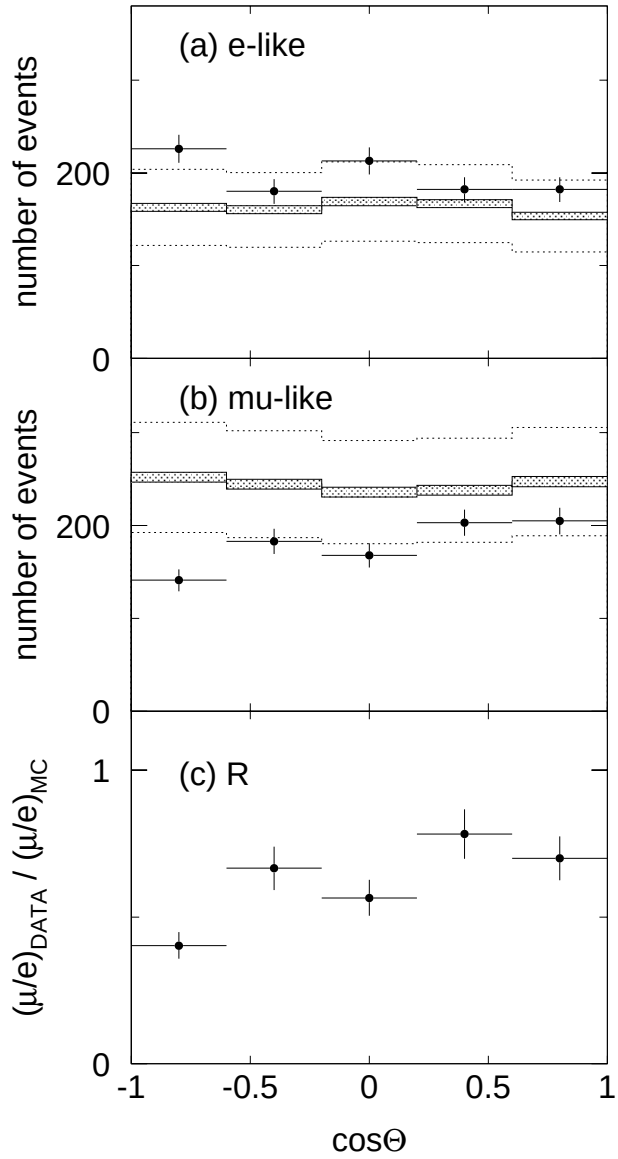

Figure 5: Zenith angle distributions for: (a) e-like events, (b) μ-like events, and (c) R. ($\cos\Theta = 1$ means down-going.) Histograms with shaded error bars show the Monte Carlo prediction with its statistical error. Dotted histograms show the $\pm 25\%$ systematic uncertainty on the absolute normalization, which is correlated between μ-like and e-like events.